JOURNAL OF COMPUTATIONAL PHYSICS 79, 436–448 (1988)

Nonoscillatory Solution of the Steady-State Inviscid Burgers' Equation by Mathematical Programming

JOHN E. LAVERY

Nasa Lewis Research Center, Cleveland, Ohio 44135

Received June 2, 1987; revised February 19, 1988

Numerical solution of the steady-state inviscid Burgers' equation $(u^2)' = 0$ on $(0, 1)$, $u(0) = g_0$, $u(1) = g_1$ $(g_0 \neq g_1)$, is considered. To obtain the physically relevant discontinuous solution of this problem, the equation is singularly perturbed by adding a small amount of viscosity: $-\varepsilon u'' + (u^2)' = 0$. A "cell-entered" finite-difference scheme that uses two points for the inviscid part and four points for the viscous part is proposed. The overdetermined nonlinear system that results is solved by a homotopy based on the Newton linearizer and a linear programming algorithm used to solve l_1 problems. Difficulties in capturing interior layers centered at node points are observed. However, the computational results for interior layers centered between node points and for boundary layers show accurate nonoscillatory solutions with discontinuities captured in one cell on both coarse and fine grids. The amount of artificial viscosity required to obtain these solutions is small $(\varepsilon \leqslant 10^{-9})$ compared to the amount of artificial viscosity required by standard methods. A partial proof of pointwise and $L_1(0, 1)$ convergence of the linear-spline interpolant of the numerical solution to the inviscid solution $\varepsilon/h \to 0$ and $h \to 0$ is given for one case.

1. INTRODUCTION

In solving systems of conservation laws, producing accurate nonoscillatory solutions that can be efficiently computed has been a persistent problem. An appreciation of the important role played by the L_1 norm and its discrete analogue, the l_1 norm, in the analysis of numerical methods for solving conservation laws has been growing [11, 14, 15, 18]. A major advance was made by Harten [8, 9], who used the L_1 norm as a guide for constructing TVD schemes (see also [13]). In these schemes, the L_1 norm guides the choice of functions and parameters but is not otherwise a fundamental part of the solution algorithm. When the L_1 or l_1 norm is accepted as a basis for the solution algorithm, the numerical problem becomes a problem in mathematical programming rather than a problem in traditional matrix algebra. The l_1 procedure presented in this paper is a first step in this direction.

We consider here the steady-state inviscid Burgers' equation

$$(u^2)' = 0 \qquad \text{on} \quad (0, 1) \tag{1.1a}$$

0021-9991/88 $3.00

with the boundary conditions

$$u(0)=g_0, \qquad u(1)=g_1 \qquad (g_0 \neq g_1). \tag{1.1b}$$

The physically relevant solution of (1.1) is the pointwise limit as $\varepsilon \to 0$ of the solution of the singularly perturbed problem

$$-\varepsilon u'' + (u^2)' = 0 \qquad \text{on} \quad (0, 1) \tag{1.2a}$$

$$u(0)=g_0, \qquad u(1)=g_1. \tag{1.2b}$$

Both standard and compact three-point central difference schemes typically produce oscillation and nonunique solutions for small ε [6, 12, 20]. We recall for the reader the severity of the oscillatory behavior by the following set of examples. Define an equally spaced mesh by

$$x_i = ih, \qquad i=0, 1, ..., n, \tag{1.3}$$

where $h=1/n$. Let u_i be the numerical solution at x_i. Discretize problem (1.1) by the three-point "node-centered" finite-difference scheme

$$\varepsilon \frac{-u_{i-1}+2u_i-u_{i+1}}{h^2} + \frac{u_{i+1}^2-u_{i-1}^2}{2h} = 0, \qquad i=1, 2, ..., n-1, \tag{1.4a}$$

with

$$u_0=g_0, \qquad u_n=g_1. \tag{1.4b}$$

System (1.4) with $n=100$ and

$$g_0=1, \qquad g_1=0 \tag{1.5}$$

was solved for $\varepsilon=10^{-k}$, $k=1, 2, ..., 10$, with initial $u_i=1-x_i$ for each ε. For boundary conditions (1.5), the inviscid solution of (1.1) is

$$u(x)=\begin{cases}1, & 0 \leqslant x<1,\\ 0, & x=1.\end{cases} \tag{1.6}$$

The exact solution of the viscous problem (1.2), (1.5) is

$$u(x)=c\tanh(c(1-x)/\varepsilon \tag{1.7}$$

for c such that $c\tanh(c/\varepsilon)=1$ (boundary layer at $x=1^-$ for small ε). Convergence of the numerical solution was deemed to have occurred when the relative l_1 error

$$\sum_{i=1}^{n-1} \frac{|u_i^{\text{cur}}-u_i^{\text{pre}}|}{|u_i^{\text{cur}}|} \tag{1.8}$$

TABLE I

Comparison of the Solution u_i of the Three-Point Node-Centered Central-Difference System (1.4), (1.5) with the Inviscid Solution (of (1.1), (1.5); "Inv. sol.") in the Boundary Layer ($n = 100$, Initial $u_i = 1 - x_i$ for Each ε).

ε \ x	0.94	0.95	0.96	0.97	0.98	0.99
10^{-1}	0.5366	0.4616	0.3795	0.2909	0.1971	0.0995
10^{-2}	1.0000	1.0000	1.0000	0.9999	0.9820	0.7321
10^{-3}	0.8589	1.1491	0.7781	1.2176	0.6329	1.3177
10^{-4}	0.3876	1.4870	0.3239	1.5027	0.2367	1.5196
10^{-5}	0.2582	5.7184	0.2115	5.7203	0.1503	5.7223
10^{-6}	0.2462	50.672	0.2011	50.672	0.1423	50.672
Inv. sol.	1	1	1	1	1	1

Note. The entries in the table are the values of the u_i.

between the current solution values u_i^{cur} and the values u_i^{pre} of the solution on the previous Newton iteration was less than $0.5 * 10^{-10}$. The u_i in the boundary layer at $x = 1^-$ for $\varepsilon = 10^{-k}$, $k = 1, 2, ..., 6$, are presented in Table I. (These results and all other computational results presented in this paper were obtained in double-precision arithmetic on an IBM 370 using the convergence criterion involving expression (1.8) described above.) The odd–even uncoupling produced by the discretization

$$\frac{u_{i+1}^2 - u_{i-1}^2}{2h} \tag{1.9}$$

of the inviscid term $(u^2)'$ is responsible for the increasing oscillation seen in the numerical results as ε goes from 10^{-3} to 10^{-6}.

At the cost of increased computing time and perhaps some bias in the discrete solution, oscillation can be reduced by using fine or stretched grids, artificial viscosity, upwinding [6, 12], or more refined schemes such as TVD and ENO schemes [8, 9, 10, 13]. The approach discussed in the present paper differs from these standard approaches. Here, a l_1 mathematical programming procedure is applied to an overdetermined "cell-centered" finite-difference system to produce a solution.

2. Cell-Centered Finite-Difference Schemes

We choose to discretize problem (1.2) on the equally spaced mesh defined by (1.3) using a four-point difference scheme for the viscous term $-\varepsilon u''$ and a two-point difference scheme for the inviscid term $(u^2)'$, both schemes being centered at the midpoint of the cell (x_i, x_{i+1}) and having second-order accuracy there:

$$\varepsilon \frac{-3g_0 + 7u_1 - 5u_2 + u_3}{2h^2} + \frac{u_1^2 - g_0^2}{h} = 0 \qquad \text{(first cell)}, \tag{2.1a}$$

$$\varepsilon \frac{-u_{i-1} + u_i + u_{i+1} - u_{i+2}}{2h^2} + \frac{u_{i+1}^2 - u_i^2}{h} = 0, \qquad i = 1, 2, ..., n-2, \text{ (interior cells)} \tag{2.1b}$$

$$\varepsilon \frac{u_{n-3} - 5u_{n-2} + 7u_{n-1} - 3g_1}{2h^2} + \frac{g_1^2 - u_{n-1}^2}{h} = 0 \qquad \text{(last cell)}. \tag{2.1c}$$

The two-point cell-centered difference scheme

$$\frac{u_{i+1}^2 - u_i^2}{h} \tag{2.2}$$

used in Eqs. (2.1) for the inviscid term $(u^2)'$ does not have the odd–even uncoupling and resulting oscillatory behavior of the three-point node-centered scheme (1.4). This type of discretization for the inviscid term, often called a "bidiagonal" scheme, has been proposed and investigated in [5, 16, 21].

While Eqs. (2.1) have the advantage of suppressing odd–even uncoupling (and doing so without upwinding or, as will be seen in Section 4, appreciable artificial viscosity), they form an overdetermined system. There are n equations for the $n-1$ unknowns u_i, $i = 1, 2, ..., n-1$. In such a situation, one tends to attempt to solve the system first by least-square fitting, which will be done in the next section. We conclude the present section with some comments on why the overdetermined nature of system (2.1) should not come as a surprise.

The inviscid problem (1.1) is overdetermined in the sense that it has no strong (continuous) solution when $g_0 \neq g_1$. System (2.1), (1.4b) is a numerical approximation of (1.2), which, for small ε, is a singular perturbation of (1.1). That (2.1), (1.4b) is overdetermined is expected, since it is an approximation of the overdetermined problem (1.1). The overdetermined nature of (1.1) is an indication that its solution should be sought in the class of discontinuous functions (weak solutions) rather than continuous functions (strong solutions). By the same token, the overdetermined nature of (2.1), (1.4b) is an indication that its solution should be sought among those functions that are effectively discontinuous on the grid being used. It will be seen in Section 3 that least-square fitting does not permit such solutions to be found. In Section 4, the l_1 algorithm that does find discontinuous solutions will be presented.

3. The Least-Square Solution Procedure

Solving system (2.1), (1.4b), (1.5) by least squares consists in finding the u_i that minimize the sum of the squares of the residuals of system (2.1),

$$\sum_{i=0}^{n-1} r_i^2, \tag{3.1}$$

where r_i is the left side (the residual) of the ith equation in set (2.1).The computational algorithm used to minimize (3.1) consisted in iteratively creating the (linear) Newton system for (2.1), (1.4b), (1.5) and solving this linear system by least squares using the IMSL (Ed. 9) subroutine LLSQF. Results were obtained for the cases $\varepsilon = 10^{-k}$, $k = 1, 2, ..., 10$, with $n = 100$. The u_i in the boundary layer for $\varepsilon = 10^{-k}$, $k = 1, 2, ..., 6$, are presented in Table II. The initial u_i were set equal to $1 - x_i$ for each ε. The final u_i equal the values of the viscous solution $u(x_i)$ given in (1.7) with absolute error $\leqslant 10^{-3}$ for $\varepsilon = 10^{-1}$. As ε decreases from 10^{-2} to 10^{-10}, however, the sharp boundary layer at $x = 1^-$ does not develop. The u_i equal $\sqrt{1 - x_i}$ with absolute error $\leqslant 10^{-3}$ for $\varepsilon = 10^{-5}$ and with absolute error $\leqslant 10^{-8}$ for $\varepsilon = 10^{-10}$.

The explanation for this behavior is as follows. As $\varepsilon \to 0$, system (2.1), (1.4b), (1.5) becomes the system

$$\frac{u_{i+1}^2 - u_i^2}{h} = 0, \qquad i = 0, 1, ..., n-1, \tag{3.2a}$$

$$u_0 = 1, \qquad u_n = 0. \tag{3.2b}$$

To solve this system by least squares is to minimize the sum of the squares of expressions (3.2a), that is, sum (3.1) with $\varepsilon = 0$. Differentiating this sum with respect to each of the unknowns and setting the derivatives equal to zero yields the nonlinear system

$$4u_i(-u_{i-1}^2 + 2u_i^2 - u_{i+1}^2) = 0, \qquad i = 1, 2, ..., n-1, \quad u_0 = 1, \quad u_n = 0. \tag{3.3}$$

The exact solution of (3.3) is $u_i^2 = 1 - x_i$ or, choosing the positive square root, $u_i = \sqrt{1 - x_i}$. It can be proved that, as $\varepsilon \to 0$, the solution u_i of the least-squares problem with nonzero ε converges to $\sqrt{1 - x_i}$ for each i (for a sufficiently close initial guess).

TABLE II

Comparison of the Least-Squares Solution u_i of the Four-Point Cell-Centered Finite-Difference System (2.1), (1.4b), (1.5) with the Inviscid Solution (of (1.1), (1.5); "Inv. sol.") in the Boundary Layer ($n = 100$, Initial $u_i = 1 - x_i$ for Each ε).

ε \ x	0.94	0.95	0.96	0.97	0.98	0.99
10^{-1}	0.5380	0.4631	0.3809	0.2921	0.1980	0.1000
10^{-2}	0.6061	0.5967	0.5824	0.5485	0.4821	0.2946
10^{-3}	0.3123	0.2964	0.2795	0.2614	0.2368	0.2081
10^{-4}	0.2493	0.2283	0.2053	0.1792	0.1481	0.1103
10^{-5}	0.2454	0.2241	0.2005	0.1738	0.1420	0.1010
10^{-6}	0.2450	0.2237	0.2000	0.1733	0.1415	0.1001
Inv. sol.	1	1	1	1	1	1

Note. The entries in the table are the values of the u_i.

The tight point-to-point coupling imposed by Eqs. (2.1) when ε is small, which effectively requires that $u_{i+1} \approx u_i$ (cf. Eq. (3.2a)), and the tendency of least-square fitting to enforce Eqs. (2.1) approximately in all cells is responsible for this unexpected result. Equations (2.1) are valid in most cells but are not even approximately valid in a "shocked" cell, that is, a cell where u undergoes a jump so large that it is perceived on the grid as a discontinuity. In such a cell, the finite-difference scheme is not a good approximation of the original equation. The desired algorithm is one that locates the shocked cell and solves the system of $n-1$ equations for $n-1$ unknowns consisting of system (2.1) minus the equation for the shocked cell. Such a method is presented in the next section.

4. The l_1 Linear Programming Solution Procedure

The l_1 procedure for solving the overdetermined system (2.1) consists in finding the u_i that minimize the sum of the absolute values of the left sides of Eqs. (2.1),

$$\sum_{i=0}^{n-1} |r_i| \tag{4.1}$$

(cf. (3.1)). The minor change in the expression to be minimized produces a radical change in the algorithm and in the solution.

References [1–4, 7, 17, 19] give information on the l_1 strategy and on linear and nonlinear programming algorithms for implementing it. A capacity to remain unaffected by outliers in the data is characteristic of l_1 procedures [7]. In the situation under consideration in this paper, this capacity translates into a capacity to permit the equation in the shocked cell not to be satisfied while requiring that the remaining equations be satisfied exactly.

Expression (4.1) was minimized by an iterative method, each iteration of which consisted in creating the Newton system for Eqs. (2.1), (1.4b), (1.5) and solving that system by the Barrodale–Roberts l_1 algorithm [1, 2], a modification of the simplex method, as implemented in the IMSL (Ed. 9) subroutine RLLAV. Convergence of the numerical solution was deemed to have occurred when the relative l_1 error (1.8) was less than $0.5 * 10^{-10}$. The program was run for $\varepsilon = 10^{-k}$, $k = 1, 2, ..., 10$, with $n = 100$ and with initial $u_i = 1 - x_i$ for each ε. Convergence occurred for $\varepsilon = 10^{-1}$ and 10^{-2} only. Excellent agreement between the u_i and the values $u(x_i)$ of the viscous solution (1.7) of problem (1.2), (1.5) was observed for these two values of ε.

Since the l_1 procedure starting from $u_i = 1 - x_i$ did not converge for $\varepsilon \leqslant 10^{-3}$, a homotopy was added. The l_1 procedure with homotopy consisted in applying the l_1 procedure described above successively for $\varepsilon = 10^{-k}$, $k = 1, 2, ...$, with the initial u_i for $\varepsilon = 10^{-1}$ being $1 - x_i$ and the initial u_i for $\varepsilon = 10^{-k}$, $k = 2, 3, ...$, being the solution for the previous (next larger) ε, namely, 10^{-k+1}. Convergence occurred for ε as small as 10^{-9}. Failure to reach a solution for $\varepsilon = 10^{-10}$ was probably due to approaching the noise level of the computer. Values of u_i in the boundary layer are

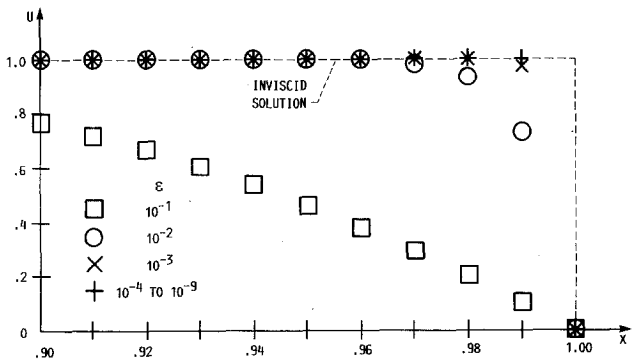

FIG. 1. Comparison of the l_1 solution u_i of system (2.1), (1.4b), (1.5) with the inviscid solution (of (1.1), (1.5)) in the boundary layer ($n = 100$, homotopy).

plotted in Fig. 1 for $\varepsilon = 10^{-k}$, $k = 1, 2, ..., 9$, and are listed in Table III for $\varepsilon = 10^{-k}$, $k = 1, 2, ..., 6$. The absence of oscillation and overshooting in all of these l_1 solutions is remarkable. The differences between the u_{99} in Table III and the inviscid solution 1 are observed to be $O(\varepsilon)$. This estimate is confirmed by the fact that u_{99} was equal to $1 - 25\varepsilon$ for $\varepsilon = 10^{-k}$, $k = 7, 8, 9$. The further the x_i is from the discontinuity at $x = 1^-$, the faster the convergence is: the numerical results for $\varepsilon = 10^{-k}$, $k = 1, 2, ..., 9$, as a whole suggest that as $\varepsilon \to 0$ the difference between u_{100-m} and the inviscid solution 1 is $O(\varepsilon^m)$.

The ability of the l_1 procedure to solve a Burgers' equation with an interior layer was also tested. The physically relevant solution of problem (1.1) with

$$g_0 = 1, \qquad g_1 = -1 \tag{4.2}$$

TABLE III

Comparison of the l_1 Solution u_i of System (2.1), (1.4b), (1.5) with the Inviscid Solution (of 1.1), (1.5); "Inv. sol.") in the Boundary Layer ($n = 100$, Homotopy).

ε \ x	0.94	0.95	0.96	0.97	0.98	0.99
10^{-1}	0.53805982	0.46317169	0.038096542	0.29219862	0.19804143	0.10000122
10^{-2}	0.99979383	0.99912672	0.99630225	0.98436307	0.93424355	0.72998509
10^{-3}	1.00000000	0.99999999	0.99999961	0.99998420	0.99936759	0.97469566
10^{-4}	1.00000000	1.00000000	1.00000000	0.99999998	0.99999374	0.99749688
10^{-5}	1.00000000	1.00000000	1.00000000	1.00000000	0.99999994	0.99974997
10^{-6}	1.00000000	1.00000000	1.00000000	1.00000000	1.00000000	0.99997500
Inv. sol.	1	1	1	1	1	1

Note. The entries in the table are the values of the u_i.

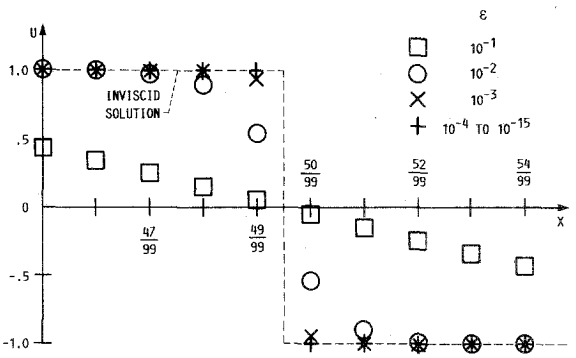

FIG. 2. Comparison of the l_1 solution u_i of system (2.1), (1.4b), (4.2) with the inviscid solution (of (1.1), (4.2)) in the interior layer ($n=99$, homotopy).

is

$$u(x)=\begin{cases}1, & 0\leqslant x<\frac{1}{2},\\ -1, & \frac{1}{2}<x\leqslant 1.\end{cases} \tag{4.3}$$

The solution of the viscous problem (1.2), (4.2) is

$$u(x)=c\tanh(c(0.5)-x)/\varepsilon) \tag{4.4}$$

for c such that $c\tanh(c/2\varepsilon)=1$ (interior layer at $x=\frac{1}{2}$). System (2.1), (1.4b), (4.2) was solved for $n=99$ (the case $n=100$ is discussed below) by the l_1 procedure with homotopy starting from $u_i=1-2x_i$. Convergence occurred for $\varepsilon=10^{-k}$, $k=1, 2, ..., 15$. Values of the u_i near the interior layer at $x=\frac{1}{2}$ are plotted in Fig. 2 for $\varepsilon=10^{-k}$, $k=1, 2, ..., 15$, and are listed in Table IV for $\varepsilon=10^{-k}$, $k=1, 2, ..., 6$. The antisymmetry around $x=\frac{1}{2}$ in the numerical solution corresponds to the antisymmetry in the inviscid solution (4.3) and the viscous solution (4.4). The data

TABLE IV

Comparison of the l_1 Solution u_i of System (2.1), (1.4b), (4.2) with the Inviscid Solution (of (1.1), (4.2); "Inv. sol.") in the Interior Layer ($n=99$, Homotopy).

ε \ x	47/99	48/99	49/99	50/99	51/99	52/99
10^{-1}	0.24810434	0.15089498	0.05064557	−.05064557	−.15089498	−.24810434
10^{-2}	0.97316110	0.88671763	0.54137960	−.54137060	−.88671763	−.97316110
10^{-3}	0.99996972	0.99877564	0.95053107	−.95053107	−.99877564	−.99996972
10^{-4}	0.99999997	0.99998775	0.99505003	−.99505003	−.99998775	−.999999997
10^{-5}	1.00000000	0.99999988	0.99950500	−.99950500	−.99999988	−1.00000000
10^{-6}	1.00000000	1.00000000	0.99995050	−.99995050	−1.00000000	−1.00000000
Inv. sol.	1	1	1	1	1	1

Note. The entries in the table are the values of the u_i.

in Table IV show that the difference between the u_i nearest the discontinuity, namely, u_{49} and u_{50}, and the corresponding values of the inviscid solution, namely, $+1$ and -1, are $O(\varepsilon)$. The numerical results for $\varepsilon = 10^{-k}$, $k = 1, 2, ..., 15$, as a whole suggest that as $\varepsilon \to 0$ the difference between u_i and the value of the inviscid solution, $+1$ or -1, is $O(\varepsilon^m)$, where m is the number of mesh units between x_i and the discontinuity at $x = \frac{1}{2}$, rounded upward to the nearest integer ($m = |i - \frac{99}{2}| + \frac{1}{2}$). On the other hand, for large ε ($\varepsilon = 10^{-1}, 10^{-2}$), there was excellent agreement between the u_i and the values $u(x_i)$ of the viscous solution (4.4).

For odd n, the discontinuity in the inviscid solution (4.3) is in the interior of a cell. The l_1 procedure, which identifies a shocked cell, performs excellently in this case. When n is even, however, the discontinuity is at a node point. This can be expected to create a problem for the procedure used here. For $n = 100$, the l_1 procedure for system (2.1), (1.4b), (1.5) with homotopy starting from $u_i = 1 - 2x_i$ produced the following results. For $\varepsilon = 10^{-1}$, the relative l_1 error (1.8) attained the value $0.6481 * 10^{-7}$ on the 6th iteration and remained there on subsequent iterations. When the calculations were cut off on the 25th iteration, the u_i coincided with the values $u(x_i)$ of the viscous solution (4.4) with absolute error < 0.0011. For $\varepsilon = 10^{-k}$, $k = 2, 3, 4, 5, 6$, the program results indicated (incorrectly) that the discontinuity was in the cell (0.61, 0.62) but otherwise produced a good solution (antisymmetric around 0.615 and nonoscillatory). For $\varepsilon = 10^{-k}$, $k = 7, 8, 9, 10$, the algorithm placed the discontinuity in the last cell (0.99, 1.00) and produced $u_i = 1$ everywhere in the interior. The reason for this behavior is as follows. The numerical solution with the discontinuity in the cell (x_{49}, x_{50}) just to the left of $x = \frac{1}{2}$, namely, the solution

$$u_i \approx \begin{cases} 1, & 0 \leqslant i \leqslant 49, \\ -1, & 50 \leqslant i \leqslant 100, \end{cases} \tag{4.5}$$

and the numerical solution with discontinuity in the cell (x_{50}, x_{51}) just to the right of $x = \frac{1}{2}$, namely,

$$u_i \approx \begin{cases} 1, & 0 \leqslant i \leqslant 50, \\ -1, & 51 \leqslant i \leqslant 100, \end{cases} \tag{4.6}$$

produce one and the same minimum of (4.1) (ε assumed small). The l_1 procedure used here, which is not equipped to handle multiple solutions, cannot decide whether to put the numerical discontinuity in the cell to the right or the cell to the left of $x = \frac{1}{2}$. In this unstable situation, the algorithm overshoots and shifts the shocked cell too far. Amending the algorithm so that it recognizes that both (4.5) and (4.6) are valid solutions will take care of this problem. The final numerical solution will be the average of these two solutions, namely,

$$u_i \approx \begin{cases} 1, & 0 \leqslant i \leqslant 49, \\ 0, & i = 50, \\ -1, & 51 \leqslant i \leqslant 100. \end{cases} \tag{4.7}$$

(Since the r_i of expression (4.1) are nonlinear, the value of expression (4.1) at solution (4.7) may actually be larger than the value of expression (4.1) at the solutions (4.5) and (4.6)!)

The ability of the l_1 procedure to perform well on coarse grids is suggested by the good performance seen above for small ε. To give some additional feeling for how robust the procedure can be on coarse grids, the program was rerun with $n=9$ and 10 instead of $n=99$ and 100. For problem (2.1), (1.4b), (1.5) (discontinuity at $x=1^-$) with $n=10$, the l_1 procedure with homotopy produced excellent solutions for $\varepsilon=10^{-k}$, $k=1,2,\ldots,15$. For problem (2.1), (1.4b), (4.2) (discontinuity at $x=\frac{1}{2}$) with $n=9$, the procedure produced excellent results for $\varepsilon=10^{-k}$, $k=1,2,\ldots,20$. For the latter problem with $n=10$, the procedure put the discontinuity in the cell (0.5, 0.6) just to the right of $x=\frac{1}{2}$ and converged for $\varepsilon=10^{-k}$, $k=1,2,\ldots,20$. The final solution it produced was $u_i=1$, $1\leqslant i\leqslant 5$, and $u_i=-1$, $6\leqslant i\leqslant 9$. Thus the procedure performed better for $n=10$ than it did for $n=100$. When compared with the results for $n=99$ and $n=100$, the results for $n=9$ and $n=10$ suggest that, in all cases of convergence to the "correct" solution, the difference between the numerical solution u_i and the inviscid solution is $O((\varepsilon/h)^m)$, where m is the number of mesh units between the node under consideration and the discontinuity, rounded upward to the nearest integer. The results for problem (2.1), (1.4b), (1.5) with $n=10$ and $n=100$, which are typical, are presented in Fig. 3. In this figure, the slopes of the error "curves" are seen to be approximately $-m$, as the relationship $|u_{n-m}-1|=c(\varepsilon/h)^m$ or, equivalently, $\log_{10}|u_{n-m}-1|=(-m)(-\log_{10}(\varepsilon/h))+\log c$ suggests. No distinction between data points for $n=10$ ($h=0.1$) and $n=100$ ($h=0.01$) is made since the points for these two cases coincide to within graphical accuracy.

A final note in this section concerns the role of viscosity in the l_1 algorithm. If the l_1 algorithm produces (in favorable cases) accurate approximations to the physi-

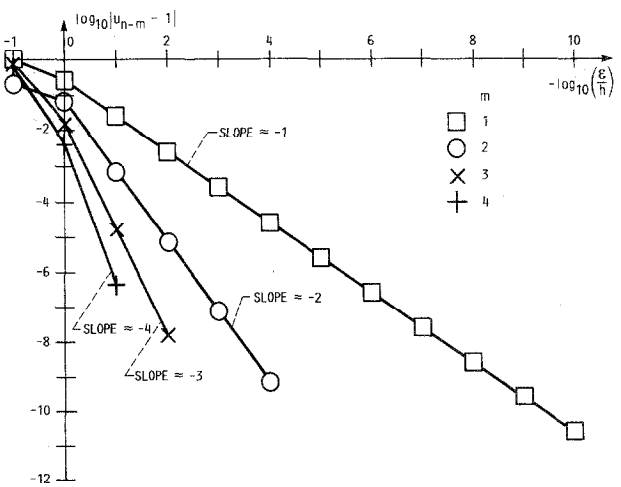

FIG. 3. Plot of $\log_{10}|u_{n-m}-1|$ vs. $-\log_{10}(\varepsilon/h)$ for problem (2.1), (1.4b), (1.5) with $n=10$ and $n=100$.

cally relevant solution of the inviscid equation for ε as small as 10^{-9}, 10^{-15}, and 10^{-20}, why not let $\varepsilon = 0$ and solve the inviscid equation directly by the l_1 procedure (just as the inviscid equation was solved in Section 3 by the least-square procedure)? The answer is that, for $\varepsilon = 0$, the minimum of (4.1), namely, $|g_0^2 - g_1^2|/h$, is attained at many solutions, including the solutions $u_i = g_0$, $i \leqslant k$, $u_i = g_1$, $i \geqslant k+1$, for any k, $1 \leqslant k \leqslant n-1$. A small amount of viscosity is the mechanism by which the l_1 procedure selects the physically relevant solution of the inviscid problem. (Viscosity is a mechanism by which the physically relevant solution can be defined in the first place—cf. [11].) In contrast to the amount of artificial viscosity required by many currently available methods for solving inviscid problems, however, the "small amount" of viscosity required by the l_1 procedure is truly small: $-10^{-9}u$" or less.

5. Convergence

The numerical results presented above demonstrate the propriety of using a l_1 procedure to solve system (2.1). It is expected that pointwise and $L_1(0, 1)$ convergence of the linear-spline interpolant of the l_1 solution of (2.1), (1.4b) to the physically relevant solution of (1.1) as $\varepsilon/h \to 0$ and $h \to 0$ can be proved using a complete search or branch-and-bound procedure for each h. One complete search involves checking a minimum of $2^n n$ solutions ($n = 1/h$). Less voluminous proofs of convergence will have to be developed. They may be constructive proofs based on nonlinear l_1 procedures developed to handle the computational side of the problem (see Section 6).

We present here a partial proof of the pointwise and $L_1(0, 1)$ convergence of the linear-spline interpolant of the l_1 solution of problem (2.1), (1.4b), (1.5) to the solution of the inviscid problem (1.1), (1.5). Assume that the shocked cell is the last cell (x_{n-1}, x_n), that is, that the l_1 procedure results in solving system (2.1) without the last equation. From this system of $n-1$ equations, create a new system of $n-1$ equations, the ith equation of which is the sum of the first i equations in the original system. In the new system, the only nonlinear term in the ith equation is u_i^2/h. Use the quadratic formula on this ith equation to solve for u_i in terms of u_j, $j \neq i$. Select the root that is asymptotically closer to 1 and approximate the square root in the quadratic formula to $O(\varepsilon/h)$. The solution of the resulting system of $n-1$ linear equations for $n-1$ unknown is

$$u_i = 1 + O(\varepsilon/h), \qquad 1 \leqslant i \leqslant n-1. \tag{5.1}$$

(The computational results mentioned in Section 4 suggest that a better result, namely, $u_{n-m} = 1 + O((\varepsilon/h)^m)$, could be achieved by a refined analysis.) Thus, pointwise convergence of the u_i to the inviscid solution 1 as $\varepsilon/h \to 0$ is established. Let v denote the linear-spline interpolant of these u_i with $v(0) = 1$ and $v(1) = 0$.

Using (5.1), it can be shown that the $L_1(0, 1)$ norm of the difference between v and the inviscid solution 1 satisfies the relationship

$$\int_0^1 |v(x) - 1|\, dx = O(\varepsilon/h) + O(h). \tag{5.2}$$

Relations (5.1) and (5.2) are statements that v converges to the inviscid solution 1 pointwise and in the $L_1(0, 1)$ norm as $\varepsilon/h \to 0$ and $h \to 0$.

At first glance, Eq. (5.2) seems to suggest that, for fixed ε, the error could become unbounded as $h \to 0$. This is not the case. The computational results for $\varepsilon = 10^{-1}$ and 10^{-2} for various h indicate that the u_i are $O(h^2)$ approximations of the viscous solution (1.7) or (4.4). The l_1 procedure thus solves not only the inviscid problem but also the viscous problem. This robustness is a distinct advantage, in spite of the fact that solving problems with significant viscosity by the l_1 procedure is expected to be more expensive than solving them by standard procedures.

6. Prospects

The formal extension of the l_1 procedure to solving systems of cell-centered finite-difference equations for steady-state and time-dependent conservation laws in one, two, and three space dimensions as well as other differential equations that have solutions with sharp layers is easily carried. out. Whether convergence will occur remains to be seen. If convergence does occur, improvements will be needed to make the procedure consistently accurate and cost-competitive with currently available methods. The Newton l_1 linear programming procedure used here can be expected to perform well only when the shocked cell identified on each step of the procedure remains one and the same for many steps in a row, which was the case in many of the numerical experiments for this paper. This procedure must eventually be replaced by nonlinear l_1 algorithms such as those in [3, 17]. Versions of these nonlinear algorithms that take into account the band structure and the fact that our systems are only slightly overdetermined will have to be developed. These versions must be able to handle discontinuities that occur at node points.

7. Conclusion

The l_1 procedure introduced in this paper produces accurate nonoscillatory solutions of the steady-state inviscid Burgers' equation. The goal of research in the near future will be to deepen the understanding of the connection between the L_1 theory and l_1 numerical procedures and to determine the classes of problems to which the synthesis of partial differential equations and mathematical programming proposed here can be applied.

REFERENCES

1. I. BARRODALE AND F. D. K. ROBERTS, *SIAM J. Numer. Anal.* **10**, 839 (1973).
2. I. BARRODALE AND F. D. K. ROBERTS, *Commun. ACM* **17**, 319 (1974).
3. R. H. BARTELS AND A. R. CONN, in Lecture Notes in Mathematics Vol. 909, edited by J. P. Hennart (Springer-Verlag, Berlin/Heidelberg/New York, 1982), p. 48.
4. P. BLOOMFIELD AND W. L. STEIGER, *Least Absolute Deviations* (Birkhäuser, Boston, 1983).
5. F. CASIER, H. DECONINCK, AND C. HIRSCH, *AIAA J.* **22**, 1556 (1984).
6. I. CHRISTIE, *J. Comput. Phys.* **59**, 353 (1985).
7. J. F. CLAERBOUT AND F. MUIR, *Geophysics* **38**, 826 (1973).
8. A. HARTEN, *J. Comput. Phys.* **49**, 357 (1983).
9. A. HARTEN, *SIAM J. Numer. Anal.* **21**, 1 (1984).
10. A. HARTEN, B. ENGQUIST, S. OSHER, AND S. R. CHAKRAVARTHY, *J. Comput. Phys.* **71**, 231 (1987).
11. A. HARTEN, J. M. HYMAN, AND P. D. LAX, *Commun. Pure Appl. Math.* **29**, 297 (1976).
12. R. B. KELLOGG, G. R. SHUBIN, AND A. B. STEPHENS, *SIAM J. Num. Anal.* **17**, 733 (1980).
13. R. J. LEVEQUE AND J. B. GOODMAN, Lectures in Applied Mathematics 22-2, edited by B. E. Engquist, S. Osher, and R. C. J. Sommerville (Amer. Math. Soc., Providence, RI, 1985), p. 51.
14. J. LORENZ, in *Theory and Applications of Singular Perturbations*, Lecture Notes in Mathematics Vol. 942, edited by A. Dold and B. Eckmann (Springer-Verlag, Berlin/Heidelberg/New York, 1982), p. 150.
15. J. LORENZ, *SIAM J. Num. Anal.* **21**, 1038 (1984).
16. R. W. MACCORMACK, *AIAA J.* **20**, 1275 (1982).
17. W. MURRAY AND M. L. OVERTON, *SIAM J. Sci. Statist. Comput.* **2**, 207 (1981).
18. B. K. QUINN, *Commun. Pure Appl. Math.* **24**, 125 (1971).
19. V. SPOSITO, W. SMITH, AND G. MCCORMICK, *Minimizing the Sum of Absolute Deviations* (Vandenhoeck & Ruprecht, Göttingen, 1978).
20. A. B. STEPHENS AND G. R. SHUBIN, *SIAM J. Sci. Statist. Comput.* **2**, 404 (1981).
21. S. F. WORNOM, *Computers & Fluids* **12**, 11 (1984).